Study of a Battery-less Near Field Communicating Sensor Network with ContactLess Simulator

David Navarro, Cédric Marchand, Laurent Carrel
Université de Lyon, ECL, INSA Lyon, UCBL, CPE
INL, UMR5270
F-69134, Ecully, France
david.navarro@ec-lyon.fr, cedric.marchand@ec-lyon.fr, laurent.carrel@ec-lyon.fr

Abstract - **Active tags and sensor nodes are an important part of the devices involved in the Internet of Things and in some cases it is impossible to power them using standard power supply or even battery. In such a case, battery-less smart sensors are needed. Design this kind of smart system is not an easy task and many different considerations must be taken into account. To face autonomy problems, battery-less sensor is a serious alternative. Energy harvesting is one of the main issue and it is mandatory to simulate the behavior of the system before designing and manufacturing it. In this article, we present ContactLess Simulator (CLS). It is developed in order to simulate contactless powered smart systems such as Near Field Communication (NFC) devices. CLS has been written using visual C# and is thus very flexible and easily portable. More precisely, this article focusses on a battery-less electronic systems: an autonomous NFC smart sensor. To design such a system, the energy budget has to be explored as the central point. CLS was developed exactly for this goal and this article describes a realistic test case to demonstrate it. The test case corresponds to a battery-less sensor node. It is composed of a microcontroller unit, a temperature sensor and a NFC circuit for communication and energy harvesting.**

Keywords-Simulation; Modelling; NFC; Sensor node; Microcontroller; MCU; Energy harvesting.

I. INTRODUCTION

This paper is an extended work of [1], about autonomous Wireless Sensor Networks energy study.

The Internet of Things (IoT) is now a well-known ecosystem, continuously growing (five times more are expected be connected in the next few years), where small and smart objects interact trough communicating networks. Even if these networks can be wired or wireless, the trend is to choose wireless communication in most cases. This is explained since small devices using wireless communications gives faster and easier installation and deployment. Among these objects, sensor nodes sense physical data in order to send information or actuate.

As shown in Fig. 1, they are usually composed of a microcontroller, a sensor, a communication device and a battery or an energy harvesting system.

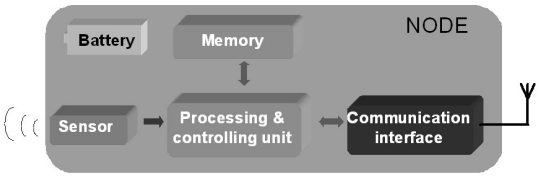

Figure 1. Typical Architecture of a smart object.

Concerning wireless communications, different solutions exist depending on the size of the network and on the communication range. Local Area Networks (LAN) are small networks whith small number of connected objects (up to few hundreds), they use short range communications (up to 300m). In this scope of networks, Bluetooth, Zigbee or Wifi are used for communication. At the contrary, Wide Area Networks are considered for big networks where more than 1000 objects are involved and where long range communication such as LoRa or mobile communications (3G, LTE, etc.) are used. Energy consumption consideration divides all these strategies of communication in two groups. The first one correspond to WAN which are often plugged with powerful supply, AC power supply or heavy acid-like battery. At the contrary, LAN and LoRa (based on the Low Power WAN) can be powered with small batteries and their autonomy can go up to years with lithium batteries and a smart usage.

It is even possible to design battery-less sensor node (energy-constrained electronic systems) in LAN and new trends target energy harvesting in the environment and smart management of this precious energy to create completely autonomous systems. We consider 2 kinds of harvesting: natural and artificial energy sources. Natural sources are directly given by the Nature, such as seismic vibrations, temperature, or solar rays. Many electronic systems are developed to consider these energy sources, such as for example Seebeck-effect systems or mini-photovoltaic panels [14]. Non-natural sources include for example machine vibrations (often coupled with piezoelectric elements [18]), ambient radiofrequency waves (through radiofrequency to continuous power converters), or magnetic fields such as wireless powering systems.

Wireless powering systems exist since several years, and are nowadays widespread in powering systems, such as inductive charging stations for smartphones [10] or vehicles wireless chargers [16]. Moreover, certain lightweight systems communicate at the same time they power the object. It is the case in RadioFrequency IDentification systems (RFID). They are composed of an emitter and a receiver, called tag. The emitter sends radiofrequency waves in order to power a tag and communicate at the same time. A classical tag answers its identification number. Near Field Communication (NFC) is based on RFID. It permits very short communications at a high frequency, in a full peer to peer mode. NFC inherits characteristics from RFID, network and smart card. It is suitable for secure communications; as an example, smartphone payment is possible with NFC.

This paper focuses on NFC battery-less objects. As Energy is the major constraint of these systems, a deep study has to be led at every stage. To achieve this goal, it is an absolute necessity to simulate the system before design and production. As these systems are electronic and communicating objects, they can be studied at different levels: low-level (hardware, software) or high-level (protocol, network). Many studies involve hardware platforms, like [3]. Low-level simulations focus on hardware or radiofrequency aspects. For example, [2] describes a MATLAB-Simulink model of a radiofrequency transceiver in order to provide a quick evaluation of the performances according to noise and non-linearity of each individual block in the transceiver. [6] and [17] present studies on the physical link (emitter, air, receiver) and radiofrequency propagation aspects. [8] gives a MATLAB Simulink NFC model for radiofrequency modulation study.

High-level simulations consider protocols, network and communication performance. RFIDSIM [9] is a more complete simulator that considers physical link and protocol. It provides a realistic physical layer and permits a multi-interface and multi-channel analysis. Others higher-level simulators focus on communication protocol and communication performance, such as the well-known NS-3 simulator. NFC models and protocol study have been developed over NS-3 [5].

However, no simulator takes the energy as the central point. A new system-level simulator, called Contact-Less Simulator [1], has been developed in order to precisely study these electronic systems from the energy point of view. This paper details this new simulator, presents new features and a real test case. CLS simulator considers energy harvesting from NFC emitter and energy balance according to the tag electrical consumption. The wireless-supplied tag is not only composed of a classical NFC circuit, but of a more complex smart system. It is possible to configure a sensor node and an application, the simulation then gives the answer if the node is well designed or not.

The rest of this article is organized as follow: Section II describes the NFC system considered in this study and details its signal transmission and typical architecture. Section III presents the simulator interface, the different possible configurations and details implemented models. Section IV describes the NFC hardware used as test case and shows simulation results. Finally, Section V concludes the paper and gives future improvement that will be included inside de simulator.

II. CONSIDERED NFC SYSTEM

A. Electronic system

A typical NFC system is composed of an emitter and a tag. It is shown in Fig. 2.

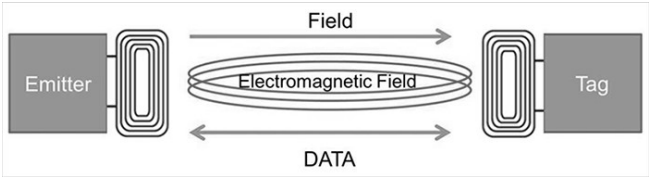

Figure 2. Typical Architecture of NFC system [13].

A tag is often composed of a NFC circuit that comprises 2 main sub-systems: energy harvesting part (for supply) and data decoding part (for communication). The energy harvesting block converts the received electromagnetic field into usable energy in order to supply the circuit. The data decoding block demodulates the signal in order to recover the bit-stream. As Energy is self-powered in passive tags, communication has to be initiated so that they are supplied in order to answer.

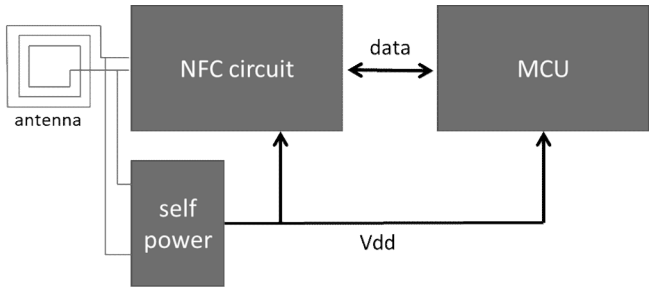

Figure 3. Classical NFC Tags

Fig. 3 shows the architecture of a classical tag composed of a microcontroller unit (MCU). When the tag is powered, the microcontroller executes the program as shown in Fig. 4.

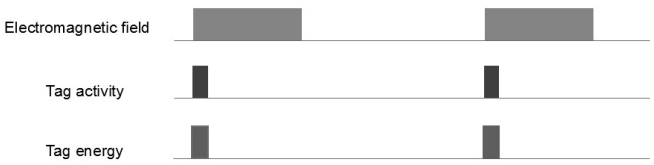

Figure 4. Classical use of NFC Tags

In this study, we consider a smarter tag comprising a microcontroller unit, a temperature sensor and a smart energy management block. Thus, this tag is called sensor node or wireless sensor node because of NFC (wireless) communications. Furthermore, we focus on a complete battery-less smart system where the only energy source comes from electromagnetic field during NFC communications between emitter and tag. We choose the ST-Microelectronics M24LR04E NFC chip for our test case. This chip is compatible with 13.56 MHz NFC ISO 15693 and ISO 18000-3 mode 1. In addition, it has an energy harvesting analog output, which makes it possible to supply other circuits on the board (i.e., microcontroller, sensor). The global considered system is shown in Fig. 2 and the tag architecture is detailed in Fig. 5.

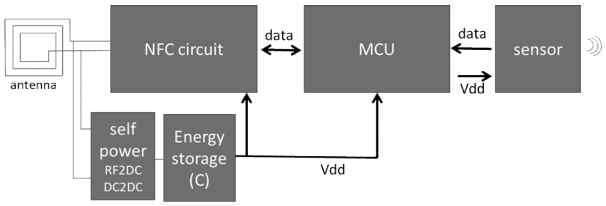

Figure 5. Considered battery-less smart tag.

The energy storage block is composed of two switches and storage capacitor as can be seen in Fig. 6. According to switches states, capacitor can charge (S1 closed, S2 opened) or discharge and supply circuits (S1 opened, S2 closed).

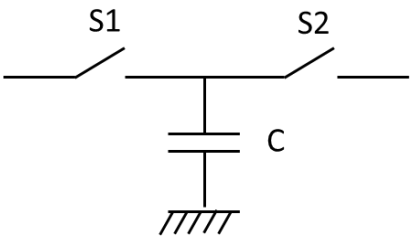

Figure 6. Energy storage block

This energy buffer offers new functionality: MCU and sensor can operate independently of NFC communications. We also target the energy use illustrated in Fig. 7. The electromagnetic field charges an energy tank, then this amount of energy is used along time by tag. Simulator will help us to check if it is possible.

Now the electronic system considered in this study has been described, the next section will provide the analysis of the signal propagation involved in such system. This will help to understand how the simulator can take into account the energy budget as the main constraint to validate a design.

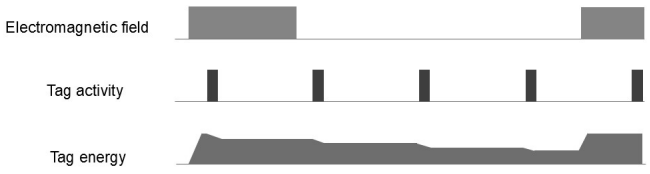

Figure 7. Targeted use of smart NFC Tag

B. Signal propagation

NFC systems use Low frequency (LF) from 125 KHz to 134 KHz, high Frequency (HF) at 13.56 MHz, or ultra-high frequency (UHF) at 860 or 960 MHz. We consider the 13.56 MHz frequency communication that is mostly used in NFC systems [13].

The emitter outputs a powerful signal in a coil (also called "antenna") at a specific -resonant- frequency. The electromagnetic field carries power and data with the help from an Amplitude Shift Keying (ASK) modulated signal [12].

Input power at receiver (tag) depends on signal strength at emitter, antennas gains, and distance between antennas. No simple exact equation exists since communication is near field and the Friis equation, which is used in classical long-range radiofrequency communications, is not valid. Indeed, Maxwell equations have to consider electric (E) and magnetic (H) fields. In our case, we use electrically small antennas. This implies that the near field limit distance r depends only on wavelength λ. This distance is given by the following equation [4], [7]:

$$r = \lambda/2\pi \quad (1)$$

As shown in Fig. 8, several kinds of radiofrequency signal propagation are observed according to the distance between emitter (represented as RFID reader and its antenna on the left) and the receiver (along the horizontal axis).

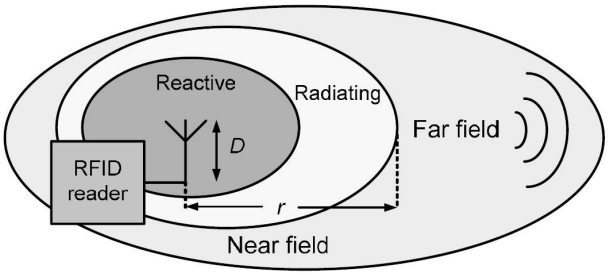

Figure 8. Radiofrequency signal propagation [14].

More precisely, the NFC system considered has frequency of 13.56 MHz and a distance between emitter and tag of few centimeters.

Thus, the tag is placed in reactive near field region leading to use simpler equations to model signal attenuation due to distance. Received power formulas are [12]:

$$P_{RX(E)} = \left(\frac{1}{k_1.d^2} - \frac{1}{k_2.d^4} + \frac{1}{k_3.d^6} \right) . P_{TX(E)} \quad (2)$$

$$P_{RX(H)} = \left(\frac{1}{k_4.d^2} + \frac{1}{k_5.d^4} \right) . P_{TX(H)} \quad (3)$$

Attenuation is also linked to pow of sixth, pow of four and pow of two of distance *d*; k1 to k5 are constants. Sometimes, simpler models are used, for example, [15] approximates power decay to be proportional to $1/d^6$.

III. CLS INTERFACE, MODELS AND SIMULATION

As it is shown in previous section, several electronic circuits compose the system. In order to provide a precise estimation of the energy consumption, it is necessary to model them separately. Models are high-level (electronic system level), they ar e written with C language.

Emitting power and antenna gain make it possible to calculate radiofrequency output power, in other terms the magnetic field H in mA/m. Frequency and distance between antennas lead to radiofrequency signal attenuation.

ContactLess Simulator (CLS) is organized as a set of configuration windows allowing the user to easily set up its system in order to launch the simulation. It has been developed in Visual C# in order to be easily portable on Microsoft 64-bit Windows operating systems. It is part of the Visual Studio Community, a free tool for academic research [11].

Graphical user interface is drawn in a horizontal way, from Emitter on the left towards Load (Electronic system) on the right. Fig. 9 shows the main windows of CLS where it is possible to recognize the global hardware architecture presented in Fig. 2. In this section, each part of CLS is described along with the model associated to each of the components of the electronic system.

A. Emitter model

The first menu in CLS (from the left) corresponds to the Field Generator (Emitter). It is modeled according to:

- Emitting power
- Frequency of the radiofrequency carrier
- Distance between emitter and tag antennas
- Emitter antenna gain

When the user enters in the Setup window of this part, a new window appears where all default meaningful values are prefilled, as shown in Fig. 10. Emitted electromagnetic field at emitter antenna and propagated electromagnetic field towards distance are calculated.

B. Tag antenna model

The emitter and tag antennas are PCB coil antennas in our prototype. Antenna gain is used to calculate propagation losses. According to above calculations, radiofrequency signal strength is known at tag antenna input. Tag antenna gain attenuation thus gives the signal after antenna. In CLS, Antenna setting, presented in Fig. 11, the tag antenna parameter is the gain (dBi). Magnetic field at tag antenna input is known from previous block. Tag antenna attenuation also decreases the signal.

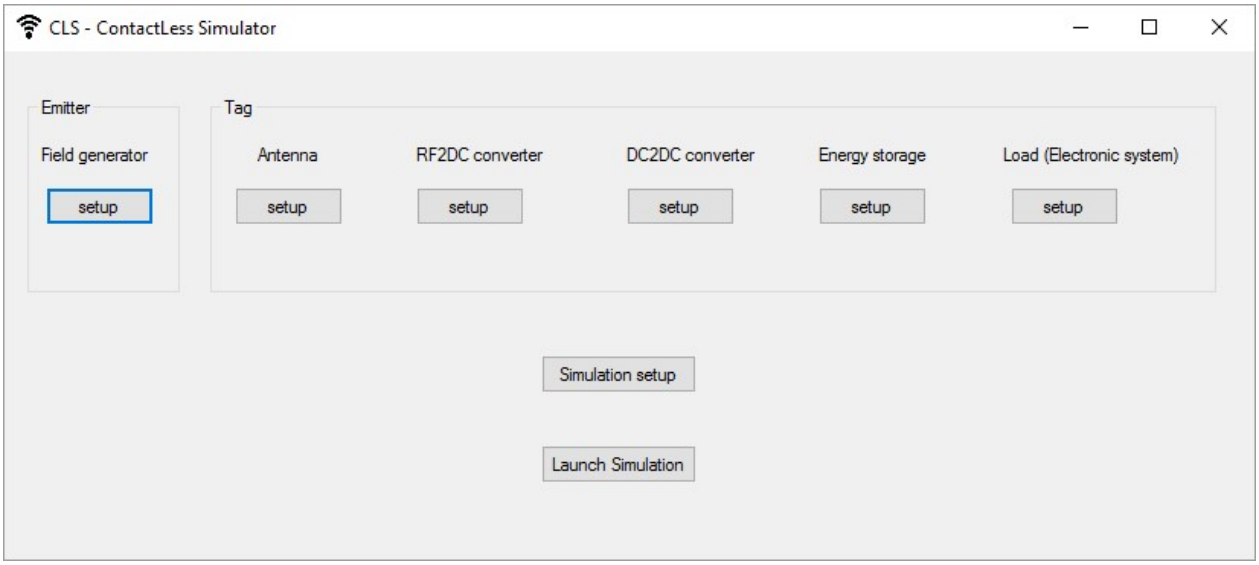

Figure 9. CLS Simulator graphical user interface

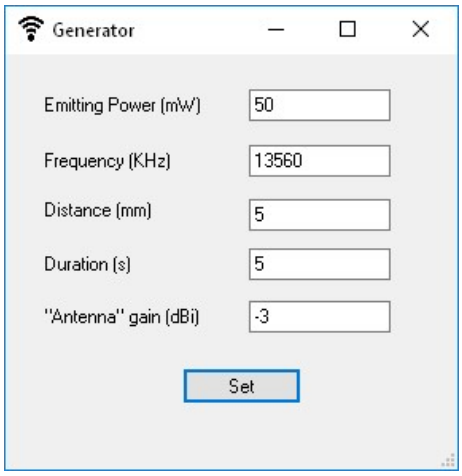

Figure 10. Electromagnetic field parameters at Emitter

Figure 11. Tag antenna parameters

C. NFC circuit model

NFC circuit has the task to demodulate the radiofrequency signal. Principle is to extract the low frequency information carried in the high frequency: the carrier. High frequency permits propagation in the medium (air, plastic packages, ...). Once the information is decoded, an answer can be send toward he emitter. Network-like communications occur in NFC. As this functionality is not the key point of this study, only the electrical consumption of this block is considered. To do this, this part is divided in two part in CLS: self-power and energy storage blocks.

D. Self-power and energy storage blocks

Several blocks in NFC circuit are considered. For a better understanding of these blocks, RF2DC and DC2DC are illustrated separately in Fig. 5. They are also modelled separately. RF2DC block receives the radiofrequency signal and converts it to a DC (voltage and current) signal. The aim is to create a power supply. Conversion goal is to extract the maximum electrical power. DC2DC block converts the RF2DC output, in order to create a usable voltage for electronic devices. Electrical power is given according to efficiency of blocks. As power is set, a good balance between voltage and current has to been chosen. Performances are based on ST-Microelectronics M24LR04E circuit characteristics. This communicating and harvesting circuit permits self-powering and provides an analog output to power other circuits in the system. Moreover, it permits data exchange between NFC circuit and microcontroller. If another circuit is to be used, global parameters, like efficiency, can be set.

1. RF2DC converter

The RF2DC part of the self-power block is shown in Fig 12. It calculates electrical power from the radiofrequency signal carrier. M24LR04E circuit has been modelled for this power conversion task. The datasheet of this circuit gives H field from radiofrequency strength and output power from H field.

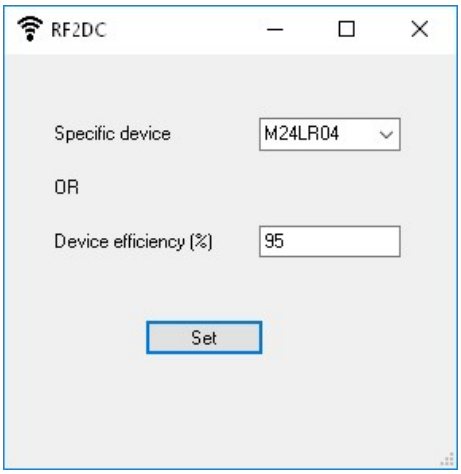

Figure 12. Radio to DC converter parameters

Then, the required current at output has to be known in order to calculate the output voltage Vout. According to the output current Isink: curves in datasheet give the output voltage the circuit can provide. For simpler use, a global parameter can be used for other circuits: the overall power efficiency (output versus input).

2. DC2DC converter

This block is presented in Fig. 13. Models have been separated because RF2DC and DC2DC blocks could be designed in separate circuits. Thus, in order to best distinguish individual performances in the system and to define parameters if they have to be designed, they are modelled in two separate blocks. DC2DC converter efficiency is expressed in percentage between output and input.

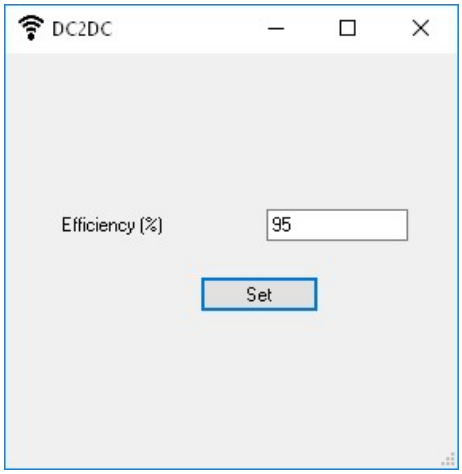

Figure 13. DC to DC converter parameters

3. Energy storage block

The energy storage parameters window presented in Fig. 14 are used to calculate the amount of energy that can be saved in an energy tank. We will later detail the novel switched capacitor architecture that is used. In Fig. 14, parameters are capacitance value (nF) and total leakages (fA) of switches and capacitor. The role of this module is to simulate the energy that can be stored (according to the power input from DC2DC bloc) and the energy that can be used (according to the supplied load and leakages). It will lead to an energy budget analysis.

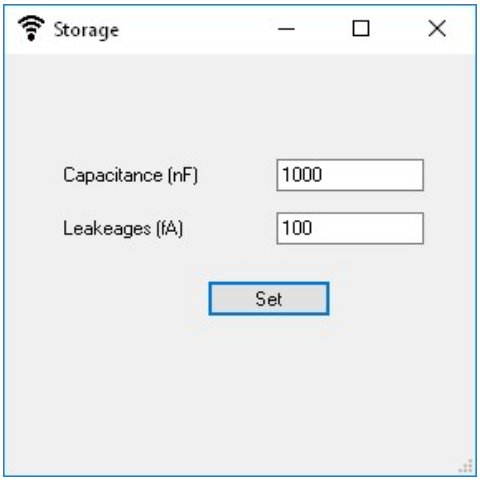

Figure 14. Load (electronic system) parameters

E. Microcontroller circuit model and sensor

For this release, microcontroller and sensor are simply modeled as an electrical load according to their activity. Microcontroller and sensor require a minimal voltage and consume a nominal current. In model, electrical power of microcontroller is calculated according to:

- Microcontroller brand and model,
- Oscillator type,
- Operating frequency.

At this stage, Microchip PIC18LF2525 is modeled. Table I shows all targeted microcontrollers that will be implemented in simulator.

TABLE I. TARGETTED MCUS MODELS

Microcontroller brand	Microcontroller model
ATMEL	ATMega-328
Microchip	PIC18LF2525
ST-Microelectronics	ST-8ML
ST-Microelectronics	STM-32
Texas Instruments	MSP-430

ATMEL, ST-Microelectronics and Texas Instruments models are under development and will be released soon. Sensor is a Maxim MAX6613 temperature sensor. Its analog output is connected to an ADC input of microcontroller. The MAX6613 is supplied with an output pin of microcontroller. Supply voltage is also the same for both components.

In this release, the load is a microcontroller unit (MCU) and a temperature sensor. When a microcontroller is chosen in the list-box, the "Configure MCU" button opens a new window. Oscillator type, operating frequency, desired supply voltage, active and sleep time of microcontroller are entered as shown in Fig. 15.

For this example, Microchip PIC18LF2525, oscillator type can be external RC (up to 4 MHz), external XTAL (crystal oscillator, up to 40 MHz), or internal oscillator. For internal oscillator, the example presented at the bottom of Fig. 15, user can select from the internal 8MHz source down to the 31KHz source.

Several frequencies are available according to frequency post-scaler in the microcontroller. Frequency (KHz) is the primary oscillator frequency that must match one possible configuration according to the oscillator type. Supply voltage of the microcontroller is then entered. All the parameters are taken from Microchip PIC18LF2525 datasheet; from current voltage versus frequency, current versus voltage and current versus frequency curves. Parameters for sensor are taken from Maxim MAX6613 datasheets.

Figure 15. Load (electronic system) parameters

F. *Simulation setup*

The simulation setup window (Fig. 16) permits to configure the simulation. The duration parameter will be used in future release in transient simulations. For the moment only static simulations are run. Design goal specifies which value is to maximize: voltage or current. Indeed, RF2DC and DC2DC blocks output a given power, and the couple voltage and current can vary. This option also configures the simulation in order to search the maximum current point or the maximum voltage point. The other parameter (for example, voltage if current is the design goal) is displayed as a result. Designer has to take it into account in design as a constraint. If the value of this other parameter is unreal, parameters concerning the hardware have to be changed, for example the microcontroller speed.

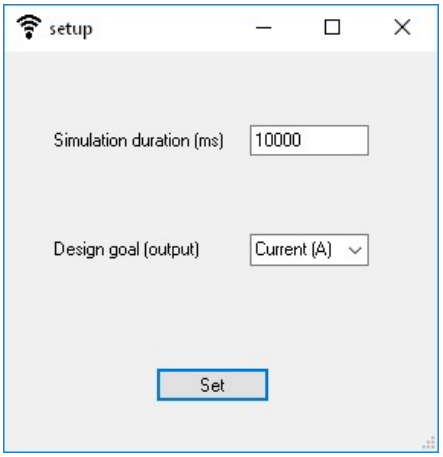

Figure 16. Simulation Setup window.

IV. TESTCASE AND RESULTS

To illustrate how the simulation behaves, a test case has been simulated. All parameters used in setup windows are summarized in Table II. Simulation time for a static analysis is configured to few milliseconds. Results are presented in Fig. 17. The left part shows results on tag side where the magnetic field H is calculated. It depends on emitter power, distance, and antennas gains. Then the harvesting part gives output of RF2DC and DC2DC parts in the M24LR04E.

TABLE II. PARAMETERS USED FOR TESTCASE SIMULATION

Emitting power	50 mW
Frequency of carrier for NFC communication	13560 MHz
Distance emitter / tag	5 mm
Duration of NFC communication	5 s
Antennas gain (emitter & tag)	-3 dBi
RF2DC & DC2DC converters	Equations from M24LR04E
Energy storage capacitance	1000 nA
Switches leakages (energy storage)	100 fA
Microcontroller brand/model	Microchip / PIC18LF2525
Microcontroller Oscillator / Operating voltage range	Internal oscillator, 31KHz / 2V to 5.5V
Sensor / Operating voltage range	Maxim MAX6613 / 1.8V to 5.5V
Duration of node sensing and MCU processing and storage	100 ms
Simulation setup	Design goal = current

As design goal of the example is the output current, the simulator calculates the nominal current to retrieve from harvesting part. Nominal current is fixed by the required current from the electrical load (MCU and sensor). This current is calculated from MCU and sensor parameters: PIC18LF2525 requires 15.05µA when running from internal oscillator at 31KHz. MAX6613 consumes 7.5µA. Simulator then calculates the harvesting possible voltage output for a sink current of 22.55µA. From datasheet curves in the model, simulation gives 2.67V. Fig. 17 shows that the required power for load is 67.64µW but the harvester can only provide 60.2µW. As a result, the required voltage 3V is not reached. Designer will have to deal with a 2.67V supply, or decrease load current consumption in order to increase supply voltage.

Energy calculations are also implemented in the simulator. It considers electrical power consumption and active time. Active time for the emitter correspond to the duration of the electromagnetic field. Result window thus displays 301µJ for 5s duration. Active time for the MCU is time while MCU is running (time running parameter in Fig. 15). Its energy is then 6.76µJ for 100ms. This result allows the designer to plan how many cycles the MCU could run with a single electromagnetic charge. It is 44 cycles for this example.

Battery-less system is also possible: for example, an application in industry where a sensor network is deployed in the aim of measuring a temperature on several machines. Each evening, a person will read the data on each sensor node with a 5 seconds NFC communication. While downloading data from node to phone (or tablet), the node is being charged for the next day: it is able to make a measurement every 33 minutes for the next 24 hours.

V. CONCLUSIONS AND FUTURE WORKS

In this article, a concrete energy analysis of novel electronics architecture and ContactLess Simulator was presented. CLS is a simulator dedicated to energy efficiency in battery-less sensor node. Its interface is based on setting windows to graphically configure a NFC system composed of an emitter and a smart tag. As targeted tags are battery-less (self-supplied), it comprises an energy harvesting module with a RF2DC and DC2DC converter, a microcontroller unit (MCU) and a sensor. Each hardware block is configured by a setup window form. Simulation can be tuned for one design goal: search maximal voltage or maximal current. This choice depends on designer priority. A launch button runs the simulation and displays a result window. Several electrical outputs are calculated: electromagnetic field at tag input, harvested power (voltage and current), harvested energy for a single contactless energy intake, required power (voltage and current) for the microcontroller and sensor, required energy for a main program loop. Result analysis on a realistic testcase shows that the harvested power is a bit weak (60.2µW) compared to the required power (67.64µW). According to the design goal, fixed to prioritize current, harvested voltage is 2.67v instead of 3v. Meanwhile, the sensing node is supplied with the required current (22.55µA). Energy calculation makes it possible to think about a better use of the energy. Indeed,

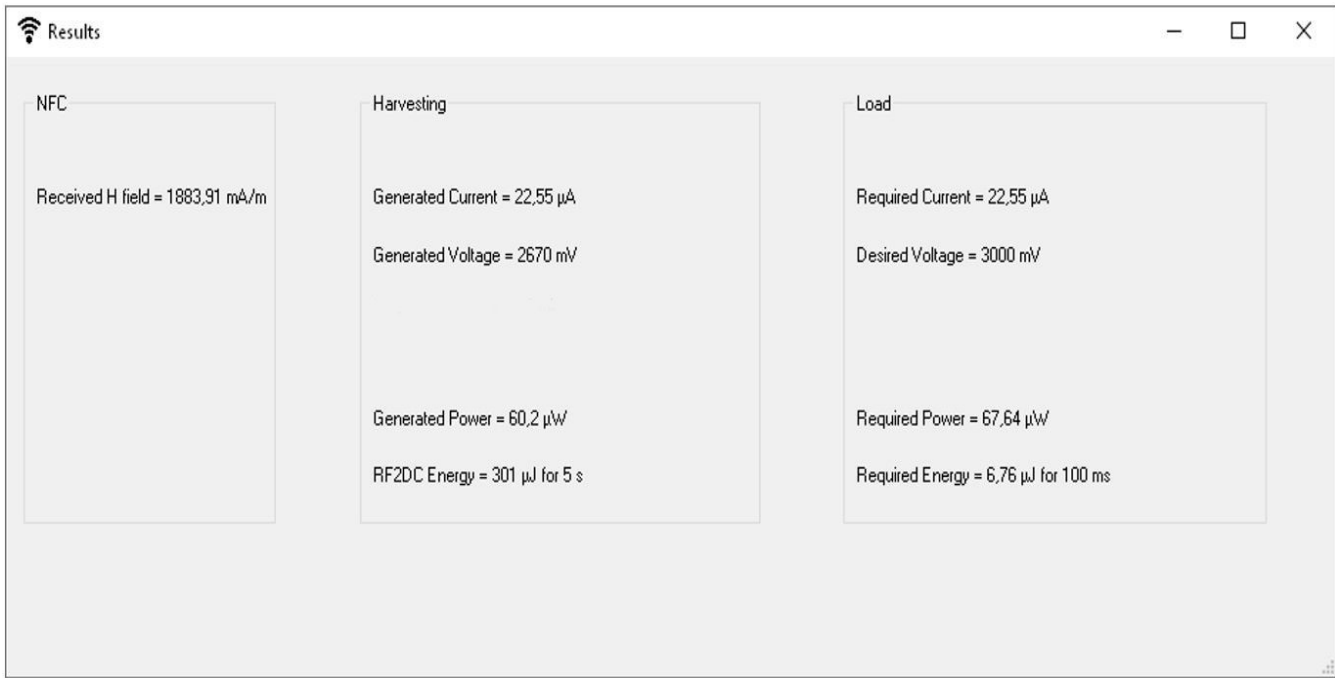

Figure 17. Result window

harvested power is weak but harvested energy (301µJ) is much bigger that required energy (6.76µJ). Feasibility is also proven: it is possible to charge the energy buffer during a 5 seconds NFC communication (while previous data are retrieved) then to use the battery-less system for 44 data recording (temperature measurements).

ContactLess Simulator can be improved to support transient analysis and to propose devices according to design constraints for example. Other microcontroller and sensor will be added and the global interface will be changed to be closer to Fig. 5. Another possible improvement will be to add curves in the results window in order to helps the designer to know understand where the sensor node can be modified to meet the constraint. Finally, it may be interesting to implement realtime static analysis to the simulator to provide an efficient support during the design phase and dedicate the simulation to transient analysis.

REFERENCES

[1] D. Navarro and G. Migliato-Marega, "Cls: Contactless simulator," in The 12th International Conference on Wireless and Mobile Communications, Barcelona, Spain, 2016, pp. 65–69.

[2] D.-K. Ahn, S.-G. Bae, and I.-C. Hwang, "A design of behavioral simulation platform for near field communication transceiver using matlab simulink," The Transactions of The Korean Institute of Electrical Engineers, vol. 59, no. 10, pp. 1917–1922, 2010.

[3] C. Angerer, B. Knerr, M. Holzer, A. Adalan, and M. Rupp, "Flexible simulation and prototyping for rfid designs," in Procceedings of the First International EURASIP Workshop on RFID Technology, 2007.

[4] Atmel, "Understanding the requirements of iso/iec 14443 for type b proximity contactless identification card. nov. 2005," Application Note, [Online, retrieved: 15th July 2017]. Available from: http://www.atmel.com/images/doc2056.pdf.

[5] G. Benigno, O. Briante, and G. Ruggeri, "A sun energy harvester model for the network simulator 3 (ns-3)," in 2015 12th Annual IEEE International Conference on Sensing, Communication, and Networking - Workshops (SECON Workshops), June 2015, pp. 1–6.

[6] T. Cheng and L. Jin, "Analysis and simulation of rfid anti-collision algorithms," in The 9th International Conference on Advanced Communication Technology, vol. 1, Feb. 2007, pp. 697–701.

[7] A. B. Constantine et al., "Antenna theory: analysis and design," MICROSTRIP ANTENNAS, third edition, John wiley & sons, 2005.

[8] J. Deckmar and A.Perez-Boutavin, "Nfc," [Online, retrieved: 15th July 2017]. Available from: https://fr.mathworks.com/matlabcentral/fileexchange/34915-nfc.

[9] C. Floerkemeier and S. Sarma, "Rfidsim - a physical and logical layer simulation engine for passive rfid," IEEE Transactions on Automation Science and Engineering, vol. 6, no. 1, pp. 33–43, Jan. 2009.

[10] U. K. Madawala and D. J. Thrimawithana, "A bidirectional inductive power interface for electric vehicles in v2g systems," IEEE Transactions on Industrial Electronics, vol. 58, no. 10, pp. 4789–4796, Oct. 2011.

[11] Microsoft, "Visual studio community," [Online, retrieved: 15th July 2017]. Available from: https://www.visualstudio.com/enus/products/visual-studio-community-vs.aspx.

[12] P. V. Nikitin, K. V. S. Rao, and S. Lazar, "An overview of near field uhf rfid," in 2007 IEEE International Conference on RFID, March 2007, pp. 167–174.

[13] G. Proehl, "An introduction to near field communications," STMicroelectronics, [Online, retrieved: 15th July 2017]. Available from: http://www.st.com/content/st_com/en/applications/connectivity/nearfield-communication-nfc.html, 2013.

[14] S. Roundy, D. Steingart, L. Frechette, P. Wright, and J. Rabaey, Power Sources for Wireless Sensor Networks. Berlin, Heidelberg: Springer Berlin Heidelberg, 2004, pp. 1–17. [Online]. Available: https://doi.org/10.1007/978-3-540-24606-0_1

[15] H. G. Schantz, "Near field propagation law a novel fundamental limit to antenna gain versus size," in 2005 IEEE Antennas and Propagation Society International Symposium, vol. 3A, July 2005, pp. 237–240 vol. 3A.

[16] R. Tseng, B. von Novak, S. Shevde, and K. A. Grajski, "Introduction to the alliance for wireless power loosely-coupled wireless power transfer system specification version 1.0," in 2013 IEEE Wireless Power Transfer (WPT), May 2013, pp. 79–83.

[17] J. Wang and D. Yang, "Design of a multi-protocol rfid tag simulation platform based on supply chain," in 2009 International Conference on Management and Service Science, Sept. 2009, pp. 1–4.

[18] W. S. Wang, W. Magnin, N. Wang, M. Hayes, B. O'Flynn, and C. O'Mathuna, "Bulk material based thermoelectric energy harvesting for wireless sensor applications," Journal of Physics: Conference Series, vol. 307, no. 1, p. 012030, 2011. [Online]. Available: http://stacks.iop.org/1742-6596/307/i=1/a=012030